International Journal of Multiphysics
Volume 19, No. 1, 2025
ISSN: 1750-9548

Required Knee Flexion Moment for Medial Unloader Knee Brace in Medial Compartment Osteoarthritis

Amirhosein Javanfar[1], Mohammadreza Azimi[2]

Department of Mechanical Engineering, Faculty of Engineering and Technology, University of Mazandaran, Babolsar, Iran[1]
Institute of Microbiology and Virology, Riga Stradins University, Riga, Latvia [2]

Corresponding author: Amirhosein Javanfar, E-mail: amirhosein.javanfar@yahoo.com, ORCID iD: 0000-0003-1396-6317

Abstract

Medial unloader braces are often developed to achieve pain elimination of the knee medial compartment. In order to prevent bone-bone contact in the knee joint, a new mechanism is designed to unload the knee based on a novel computational procedure for the first time. As the knee flexion-extension moment has a high impact on tibiofemoral contact force, we use the procedure that calculates the cartilage penetration depth and the force in the patellar tendon simultaneously which are the main parameter for applying computational knee flexion-extension torque. Therefore, the new unloader brace applies computational knee flexion-extension torque, then it decreases the penetration depth by the novel brace to eliminate pain in knee osteoarthritis. We calculate the instantaneous center of rotation of the knee and design a new flexion hinge for tracking the desired instantaneous center of rotation reducing unwanted forces. The novel brace flexion hinge tracks the instantaneous center of rotation accurately. Moreover, the flexible cord is designed to apply extension torque. It concluded that the 36.25 Nm of the extension moment leads to 0.3 mm cartilage penetration depth reduction. The embedded mechanism applies knee extension moment by the flexible cord to support assistive extension moment with the maximum amount of 1375 N. Finally, by computing the magnitude of knee flexion-extension torque, we know the relation between compensated moment applied by the brace and tibiofemoral contact force reduction for the first time.

Keywords: Knee dynamics; Musculoskeletal modeling; Contact model; Cartilage penetration depth; unloader brace; Flexion extension moment.

1. Introduction

Knee bracing may reduce pain and disease progression, thereby postponing the need for joint replacement [1] by unloading the internal knee contact forces (CF) in the affected area via applying external loads and moments [2]. As a non-invasive treatment of KOA, the literature contains diverse conclusions [3], which may be due to the predominant focus on reducing the external knee adduction moment (KAM) [1-2, 4-5]. KAM is often considered a surrogate measure of the medial CF [6–8]. Walter et al. noted that KAM lessening in vivo might not guarantee a reduction of the internal loads on the medial compartment [7]. Noticeably, medial thrust gait is prone to increase the knee flexion-extension moment (KFM), which may debilitate the assistance of reducing the KAM [15]. The same trend is observed, where knee flexion-extension moment (KFEM) had a high impact on the first peak of CF [8]. To assist and empower muscles, providing a KFEM, moment actively [9–12] or quasi-passively [13–14] might be considered within exoskeleton technology.

Rarely have we seen that the brace exerts both KAM and KFEM simultaneously. The inspiring evolved brace, Levitation (Springloaded Technology, Helifax, Canada), is not only assigned to support the quadriceps role but also equipped to provide the tricompartment unloading effect [15]. However, at the peak flexion angle, the Levitation brace applies approximately 11 Nm KAM [15]. It could have a negative effect on toe clearance and muscle co-contractions. Therefore, the design process in [8] is developed through a quasi-passive prototype. It targets the first CF peak during gait without interference during the swing phase. Recent studies [8, 15-16] concentrate on applying torque respecting knee behaviour in the gait cycle computationally to unload the knee adaptively.

Moreover, the human knee joint is assumed as one degree of freedom revolute joint, but the knee instantaneous center of rotation (ICR) moves like a polycentric joint. A relative sliding motion is generated (pistoning) between the device and the leg by bracing a single-axis device joint on the multi-axial human knee joint [17]. Pistoning leads to sliding motions and creates residual forces on the leg. Due to the sliding motion, patients confront the inconvenience. Hence the binding forces applied by straps that oppose the sliding motion cause pain. The phenomenon can be eliminated by an adaptive joint which mimics the motion of the knee center [18]. Commonly, polycentric knee joints with gears or cam-follower type mechanisms are applied to mimic the ICR [18-19].

If the patient uses the orthosis, the proper knee model [20-22] for cartilage contact description [23-24]; location of the contact points, and ligament and tendon force [25] will be preferred to calculate the mechanical parameters of knee [26]. Therefore, the model in [24] assists us to present the relation between compensated moment applying by brace and tibiofemoral contact force reduction for first time. Then, brace flexion-extension torque is calculated to reduce the tibiofemoral contact force. Based on the new relation in this study, it is clear that what the magnitude of contact force is reduced by applying brace flexion-extension torque. Moreover, our designed brace with the double hinge assists us to prevent unwarranted rotation from adduction to abduction which it oblige the knee to confront the overloading of the lateral compartment [27].

2. Objectives

As the lack of relation between the cartilage penetration depth and extension moment, there are not any studies to apply extension moment eliminating pain computationally. The innovative framework that can calculate the cartilage penetration depth assists the novel brace to be discriminated from current braces exclusively. The distinguishing attribute is applying computational knee flexion-extension torque to prevent the critical threshold of δ. The proposed dynamic unloader system can triumph over the challenges. The contributions of this paper are listed below:

- Presenting a relation between the compensated extension moment applying by brace and reduced tibiofemoral cartilage penetration depth for first time
- Designing and evaluating the novel hinge for the knee brace applying knee flexion-extension torque to avoid the critical threshold of δ respecting ICR.

3. Methods

Fig. 1 symbolizes the overall design of the knee brace. Here, the levitation brace, one of the best unloader ones, and our brace design with a dynamic continuous unloader is illustrated. We promote the potential of the brace in this field by adding flexible cord to apply flexion-extension torque. This proposal can significantly boost the reliability of the brace in the unloading role and eliminate pain in KOA. Therefore, the schematic of the system applicable to various braces is depicted in Fig. 1. Moreover, an embedded mechanism (designed double-hinge) is demonstrated in Fig. 1. The control mechanism is a key element of the brace to alter the knee abduction-adduction angle (KAAA) continuously explained by detail in [27].

In compared braces [15, 28] of Fig. 1, the amount of flexion-extension torque is not computational based on cartilage penetration depth and bone-bone contact. The following sections clarify that how the novel knee brace design assists us to knee unloading process. Then the motion of knee brace is evaluated to track the ICR. Moreover, the flexion-extension torque of the brace in sagittal plane is calculated based on the knee model [29].

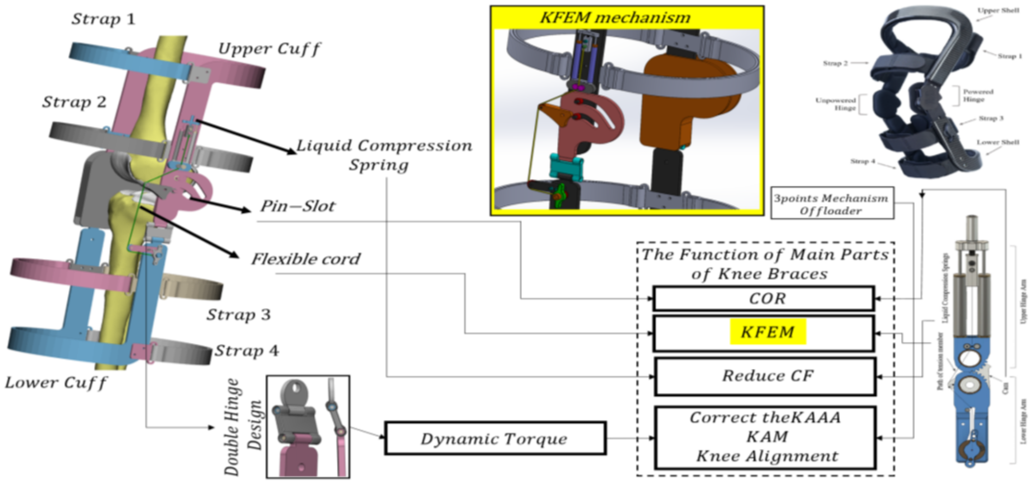

Fig.1. Schematic of designed brace with embedded KAAA control mechanism hinge (double-hinge) and flexible cord comparative with typical unicompartment tibiofemoral osteoarthritis (TFOA) offloader brace [28] and Tri-Compartment Unloader [15] (yellow areas represent our proposed embedded mechanism in the present study)

The proposed design not only supports joint reaction force (via liquid compression spring) like levitation brace but also tracks ICR by a new flexion hinge, and applies a dynamic extension torque. Moreover, the dynamic abduction torque is applied to correct the KAAA. Hence, it may boost the safety of interaction. In this proof-of-concept study, the brace linked to the knee is simulated during the gait cycle. The brace components are designed accurately, and their function is checked in SolidWorks 2016 (Dassault Systèmes, Vélizy-Villacoublay, France) motion study.

The double-hinge mechanism as the embedded hinge is designed to distribute the joint reaction force to the tibia surface in the frontal plane, as depicted in Fig. 2. During walking, the knee was expected to have up to 4 degrees of adduction and 4 degrees of abduction [30]. The designed hinge can correct this degree of freedom of the knee, while previous braces [15] typically have no DOF in the frontal plane. The double-hinge mechanism, including revolute dampers and mechanical hard stops, is added to the brace to control the KAAA. The mechanism was explained by detail in [27].

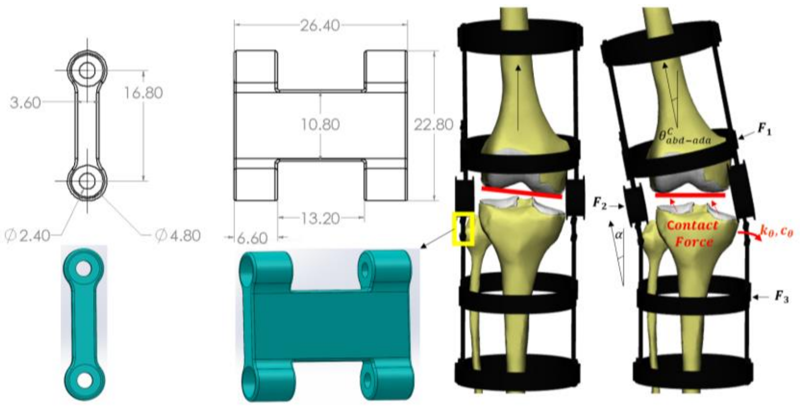

Fig.2. Schematic of attached brace to tibia-femur joint and double hinges by detail (red line shows alterating KAAA, α: double-hinge angle, $\theta^{C}_{abd-ada}$ is the separation angle) [27]

The main rule of the brace flexion hinge design is that the hinge should follow the ICR during gait. If the brace's mechanism does not strictly follow the ICR of the knee, it will cause additional force in the assistive device. There are some mechanisms using the four-bar linkage mechanism [31-32], two 6-link one-degree-of-freedom mechanisms [33], and geared five-bar linkage mechanism [34] to track ICR which are not simple to manufacture. These mechanisms generate inertial forces and uncontrolled flexion moment. Hence, they are not reliable in function. However, our mechanism provides the unloading force without any inertial forces and flexion moment, because the contact force of pin-slot transmit through the ICR.

One of the main goal of the present study is to simulate 3D knee movement with respect to use the data in [30] to extract ICR of knee and design the hinge. First, the knee geometry are extracted. Second, the normal knee movement is simulated respecting the defined axes. Third, a computer graphics program is written to optimize hinge motion. In the new design, the motion was defined by a pin-in-slot.

The optimum slot shape function is extracted. The body consisted slot that is attached to the lower cuff by the double hinge. Fig. 3 shows the difference between the knee and brace upper cuff ICR. Computer graphics program assist us to extract determined point to construct the slot curve tracking knee ICR proportionally. Moreover, the brace apply knee extension moment by using springs to tension the flexible cord that passes over the pin-slot to rotate the upper cuff of the brace relative to the lower cuff. The Table. 1 explains the advantages of our design in comparison of study [15].

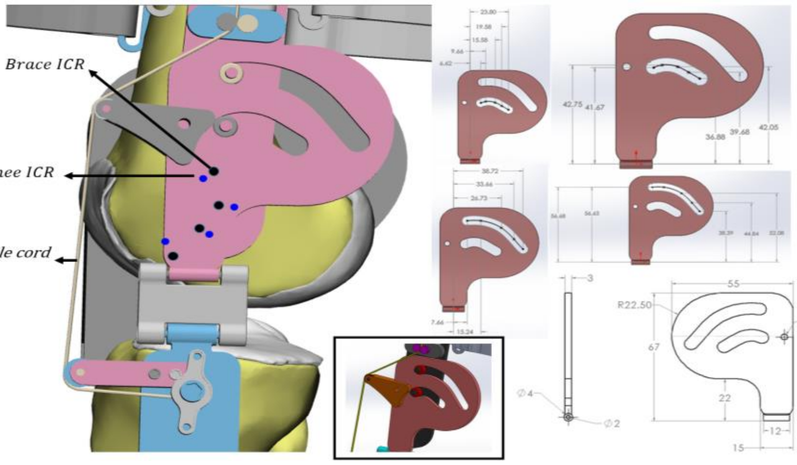

Fig.3. Schematic of knee ICR and brace lower cuff ICR during gait cycle and the slot shape definition with determined point by computer graphics program

Table.1. Comparison between our brace design and developed levitation brace by Budarick [15]

Study	Exoskeleton	Knee model	Apply flexion moment	Contact consideration in design	DOF in KAAA	Gliding motion consideration in design	ICR	Gait analysis
Budarick (2020) [15]	Knee Brace	Rigid Hinge	✓	×	×	×	×	×
Present study	Knee Brace	Compliant knee model	✓	✓	✓	✓	✓	✓

One of the most requisite processes in KOA bracing is the relation between mechanical parameters, particularly KFEM and CF. Therefore, characterizing the parameters contributing to the medial contact force can potentially find more effective therapeutic interventions to slow down progression [34].

We consider δ for the relation that can correlate the medial compartment's unloading to KFEM. It is necessary to make a relation between medial δ, and KFEM. Therefore, the equation of motion according to the Multibody system dynamic attitude is used to achieve the knee mechanical parameters. This is the first study that presents the equation which states the correlation of KFEM, MCF (medial contact force), with δ.

Contact models are essential in the dynamic behavior analysis of mechanisms and practical case studies [25-30]. To calculation of MCF according to the study [41], the δ is the point of maximum penetration depth in collision geometrical conditions can be obtained as [41]

$$\begin{cases} for\ p_c \rightarrow n \parallel n' \parallel y\ , \quad t \parallel t' \parallel x \\ \qquad for\ p_c \rightarrow n \parallel n' \parallel d \end{cases} \tag{1}$$

Then δ on contact point (p_c) is used in proposed model based on the concept of viscoelastic two-layer collision modeling, can be recast as follows [41]:

$$F_{TN} = \begin{cases} K_1\delta^n + B_c(\delta)\dot{\delta} & if\ \delta \le h_{s_1} \\ K_1 h_{s_1}^n + K_2\left(\delta - h_{s_1}\right)^n + B_c(\delta)\dot{\delta} & if\ \delta > h_{s_1} \end{cases} \quad (2)$$

where K_1 and K_2 are the general stiffnesses of the first (cartilage) and second layers (bone). $B_c(\delta)$ is the parameter used to define the viscosity of the contact between the tibiofemoral articulating cartilage. The cartilage thickness in KOA, h_{s_1}, is the critical penetration depth.

Dynamic loading within human musculoskeletal forces in the gait cycle can benefit the joint unloading treatment process. In this case, inverse dynamics simulation in OpenSim (V.3.3, SimTK) is used to combine with a suitable dynamics contact model (section 3.1) as depicted in Fig. 4.

The authors prove that by controlling the proposed knee model in the sagittal plane [41], a force could be applied at the reference point of the femur. A forward dynamics modeling was presented for the femur to freely translate and rotate with 3 DOF, resulting in a dynamics system. However, two degrees of freedom of the system were constrained as the flexion-extension angle and Anterior-posterior translation shown in Fig. 4. The inputs of the knee contact model in [41] were anterior-posterior translation, flexion-extension angle (θ_ζ), net joint reaction force (f_{knee}) and the moment (n_{knee}). All externally applied moments-of-force on the knee are derived by OpenSim analysis. Moreover, the essential output was δ assisting us in calculating the assistive extension moment investigated in the following section (section 3.3).

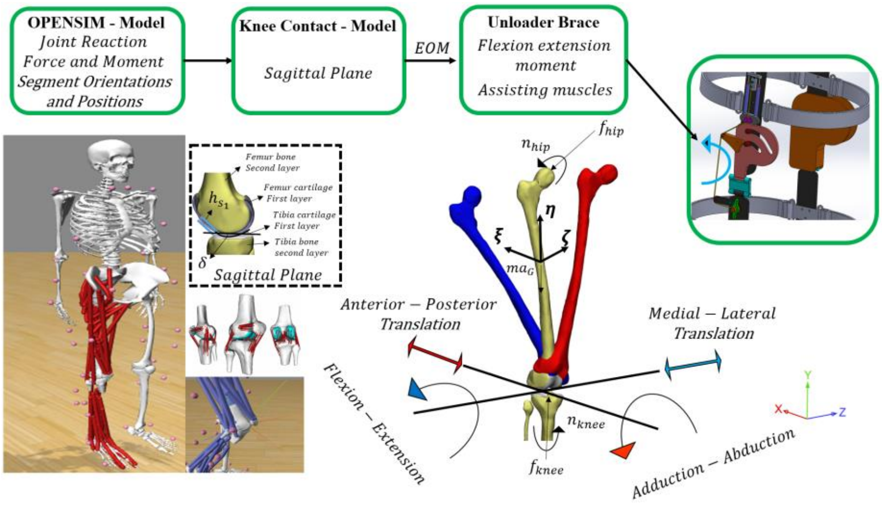

Fig. 4. Workflow of the model developed

The tibio-femoral contact point (C) was chosen as the origin for the calculation of moments. For the tibia in a free body diagram and in a static situation (Fig. 5), the moment (M) about C can be determined as [29]:

$$M = de \times f_{et} + df \times f_{ef} + dm \times mg \quad (3)$$

where f_{et}, f_{ef} and mg are the external forces acting on the tibia and de, df, and dm are their moment arms. The force in the patellar tendon (F_p) is given by:

$$F_p = \frac{M}{dp} \quad (4)$$

where dp is the moment arm of F_p. As depicted in Fig. 5, the vector equation can be written as:

$$F_p + F_{ct} + F_s + F_{et} + F_{ef} + mg = 0 \tag{5}$$

Projecting Eq. 5 in the normal (or F_{ct}) direction of the tibial plateau, the F_{ct} is:

$$\begin{aligned} F_{ct} &= F_p \times cos\beta + F_{et} \times sin\delta_1 \\ &\quad + F_{ef} \times sin\delta_2 - mg \times sin\delta_3 \\ &= 0 \end{aligned} \tag{6}$$

In tangential (or F_s) direction, the F_s is:

$$F_s = F_p \times sin\beta - F_{et} \times cos\delta_1 - F_{ef} \times scos\delta_2 - mg \times cosn\delta_3 = 0 \tag{7}$$

where δ_1, δ_1 and δ_3 are angles in relation to tibial plateau. To unloading tibiofemoral joint, the new brace applying KFEM, reduce F_p according Eq. 4. Therefore, Eq. 6 can be recast as follows:

$$F_{ct} = (\frac{M - T_{brace}}{dp}) \times cos\beta + F_{et} \times sin\delta_1 + F_{ef} \times sin\delta_2 - mg \times sin\delta_3 = 0 \tag{8}$$

According to Eq. 8, and the unloading force (F_{unload}) calculated from KOA analysis during gait cycle [41], the extension moment (T_{brace}) should be applied by the new brace is:

$$T_{brace} = \frac{F_{unload} \times dp}{cos\beta} \tag{9}$$

where T_{brace} is the assistive external torque to the ICR of knee provided by embedded flexible cord implemented in the novel brace to reduce the assisted patellar tendon force, and can be recast as follows:

$$T_{brace} = \frac{F_{unload} \times dp}{cos\beta} \tag{10}$$

where F_{fc} is the flexible cord tension force and R_{ICR} is moment arm of the tension force.

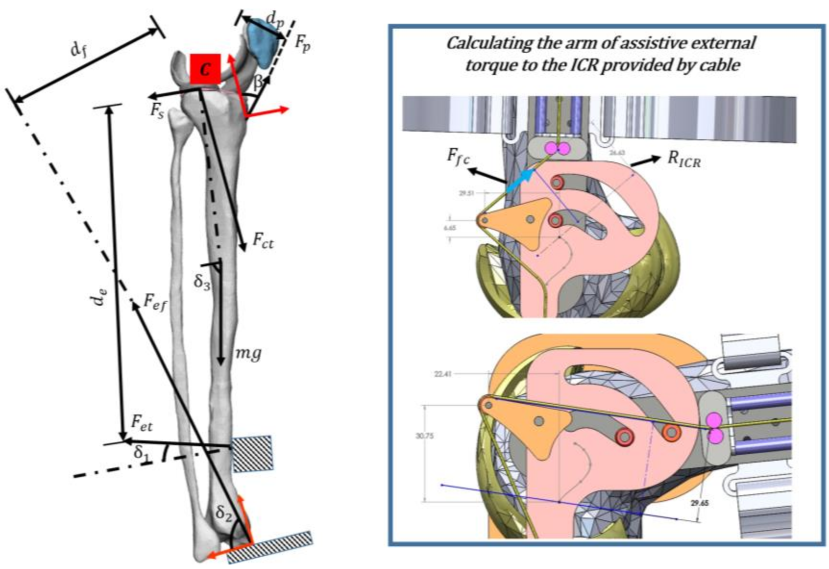

Fig. 5. Free body diagram of lower leg and brace. The magnitudes of the patellar tendon force (F_p), tibiofemoral shear (F_s) and compressive force (F_{ct}) can be calculated (see equations above) if the external forces (F_{et}, F_{ef} and mg), their angles in relation to the tibial plateau (δ_1, δ_1 and δ_3) and their moment arms (de-and df) have been determined.

4. Results

We used the proposed computational method, considering contact force and penetration depth. We calculate the unloading force for a subject with 75% KOA [35, 36]. As calculated in [36], the amount of medial penetration depth for 75% KOA is illustrated in Fig. 6. Table 2 shows the reduction of medial contact force according to the contact model [37-40] for several amount of T_{brace} (their peaks are 25.18, 36.25, and 57.54) compared with unbraced mode (normal mode). All three modes prevents the bone-bone contact and the second mode with 36.25 Nm presents an intermediateT_{brace}. The unloader force is depicted in Fig. 7 for three cases. According to unloader force, the amount of assistive external torque is demonstrated in Fig. 8 for three cases. Fig. 9 illustrates the force of the tension member (F_{fc}) of the novel brace for three cases. The force in the patellar tendon (F_p) is reduced after applying assistive external torque (T_{brace}) by the tension member.

As an advantage of the procedure, The MCF is decreased through the amount of T_{brace}, the medial penetration depth will not exceed the critical threshold of itself (0.5mm) which can be seen in Fig. 6 (the indentation for the case of OA knee with unloader). The maximum amount of the force of the tension member is about 1375N when the knee locates at the second peaks of CF.

Table.2. Difference in peak of Design Specification parameters between the Different Brace Conditions

Brace mode	***Medial Compartment Load (N) Second Peak***	***Change (%)***	***Penetration Depth Second Peak (mm)***	***Change (%)***	***Unloading of Medial Compartment (N) Second Peak***	***Flexion Moment Second Peak (Nm)***	***Flexible cord tension force Second Peak (N)***
Unbraced	941	-	0.52	-	0	-	-
Case 1	804	14.5	0.47	9.5	591	25.18	951.7
Case 2	751	20	0.45	13.5	852	36.25	1375
Case 3	663	29.5	0.4	23	1350	57.54	2175

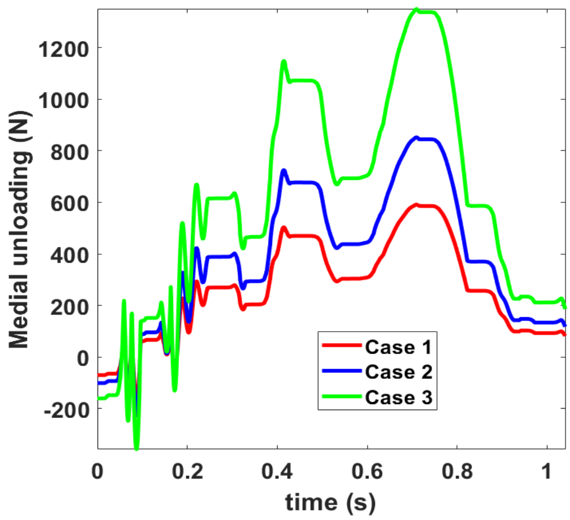

Fig.7. Medial unloading for three cases.

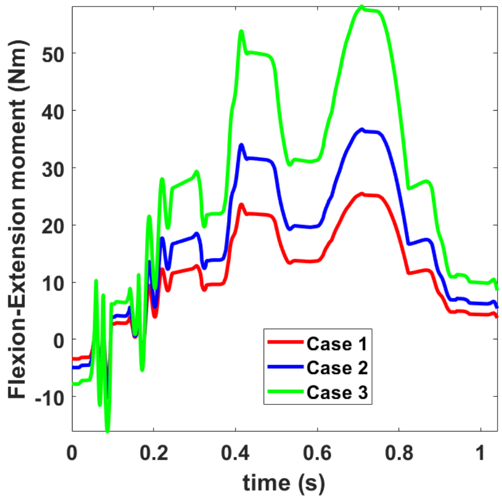

Fig.8. The required brace flexion moment (T_{brace}) applied to the femur for three cases

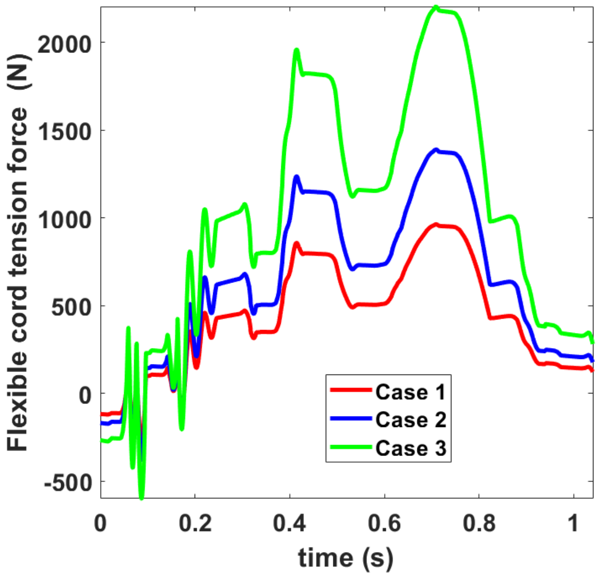

Fig.9. The required flexible cord tension force (F_{fc}) for required brace flexion moment (T_{brace}) for three cases

Our computational method via the brace design concept can support the knee to achieve these phenomena, such as unwarranted extension moment (by flexible cord), unfavorable alteration of KAAA (by double hinge [27]) and bone-bone contact (by computational procedure).The novel brace design can satisfy the goals with an important embedded flexible cord tension member to unload knee medial compartment. In comparison, the novel brace can generate continuous KFEM along with dynamic torque and supports cartilage-cartilage contact. Subsequently, the brace can be equipped based on the adaptive attitude to triumph over all the noticeable shortages that disturb the critical roles of other knee components, such as fluid synovial, ligament, and meniscus.

5. Conclusions

This brace mechanism design is based on the proposed computational method for reducing medial compartment load in osteoarthritis correlated to contact point, and cartilage penetration depth. Accordingly, the innovative framework was introduced to extract the biomechanical parameters of the knee and control the cartilage penetration depth. We realized that there are some obstacles in order to clarify the relation between the cartilage penetration depth and medial contact force and KFEM. Therefore, the proposed computational strategy streamlined the protecting process of the KOA with the unloader brace.

The proposed flowchart based on the developed algorithm for contact dynamics of planar multibody systems was implemented in a nonlinear control code using the derived equations and control approach. This study suggests significant improvement in the design procedure needed to restore normal knee function. The bone-on-bone contact could be successfully avoided by controlling the cartilage penetration depth through a control method.

To evaluate the performance of the procedure, analysis is done. Finally, we can determine the computational amount of the flexible cord tension force (maximum amount 1385N) and correlated brace extension moment (peak of extension moment 36.32N) for 75% KOA. Apparently, there are some limitations in our proposed model in terms of considering the menisci, synovial fluid, and 3D modeling. Although the embedded mechanism design might apply to different braces, the influence of muscle activations on knee moments is a crucial parameter that changes when it is adjusted to the knee.

Refrences

[1] P. Marisami and R. Venkatachalam, "Towards optimal toe-clearance in synthesizing polycentric prosthetic knee mechanism," Computer Methods in Biomechanics and Biomedical Engineering, vol. 25, no. 6, pp. 656-667, 2022.

[2] K. S. Brooks, "Osteoarthritic knee braces on the market: a literature review," JPO: Journal of Prosthetics and Orthotics, vol. 26, no. 1, pp. 2-30, 2014.

[3] J. Richard Steadman, K. K. Briggs, S. M. Pomeroy, and C. A. Wijdicks, "Current state of unloading braces for knee osteoarthritis," Knee Surgery, Sports Traumatology, Arthroscopy, vol. 24, no. 1, pp. 42-50, 2016.

[4] W. Petersen et al., "Biomechanical effect of unloader braces for medial osteoarthritis of the knee: a systematic review (CRD 42015026136)," Archives of orthopaedic and trauma surgery, vol. 136, no. 5, pp. 649-656, 2016.

[5] Y. Dessery, É. L. Belzile, S. Turmel, and P. Corbeil, "Comparison of three knee braces in the treatment of medial knee osteoarthritis," The Knee, vol. 21, no. 6, pp. 1107-1114, 2014.

[6] A. Baliunas et al., "Increased knee joint loads during walking are present in subjects with knee osteoarthritis," Osteoarthritis and cartilage, vol. 10, no. 7, pp. 573-579, 2002.

[7] J. P. Walter, D. D. D'Lima, C. W. Colwell Jr, and B. J. Fregly, "Decreased knee adduction moment does not guarantee decreased medial contact force during gait," Journal of orthopaedic research, vol. 28, no. 10, pp. 1348-1354, 2010.

[8] J. S. Stoltze et al., "Development and functional testing of an unloading concept for knee osteoarthritis patients: A pilot study," Journal of Biomechanical Engineering, vol. 144, no. 1, 2022.

[9] J. E. Pratt, B. T. Krupp, C. J. Morse, and S. H. Collins, "The RoboKnee: an exoskeleton for enhancing strength and endurance during walking," in IEEE International Conference on Robotics and Automation, 2004. Proceedings. ICRA'04. 2004, 2004, vol. 3: IEEE, pp. 2430-2435.

[10] K. Knaepen, P. Beyl, S. Duerinck, F. Hagman, D. Lefeber, and R. Meeusen, "Human–robot interaction: Kinematics and muscle activity inside a powered compliant knee exoskeleton," IEEE transactions on neural systems and rehabilitation engineering, vol. 22, no. 6, pp. 1128-1137, 2014.

[11] C. A. McGibbon, S. C. Brandon, M. Brookshaw, and A. Sexton, "Effects of an over-ground exoskeleton on external knee moments during stance phase of gait in healthy adults," The Knee, vol. 24, no. 5, pp. 977-993, 2017.

[12] M. K. Shepherd and E. J. Rouse, "Design and validation of a torque-controllable knee exoskeleton for sit-to-stand assistance," IEEE/ASME Transactions on Mechatronics, vol. 22, no. 4, pp. 1695-1704, 2017.

[13] K. Shamaei, A. A. Adams, M. Cenciarini, K. N. Gregorczyk, and A. M. Dollar, "Preliminary investigation of effects of a quasi-passive knee exoskeleton on gait energetics," in 2014 36th Annual International Conference of the IEEE Engineering in Medicine and Biology Society, 2014: IEEE, pp. 3061-3064.

[14] A. Collo, V. Bonnet, and G. Venture, "A quasi-passive lower limb exoskeleton for partial body weight support," in 2016 6th IEEE International Conference on Biomedical Robotics and Biomechatronics (BioRob), 2016: IEEE, pp. 643-648.

[15] A. R. Budarick, B. E. MacKeil, S. Fitzgerald, and C. D. Cowper-Smith, "Design evaluation of a novel Multicompartment unloader knee brace," Journal of Biomechanical Engineering, vol. 142, no. 1, 2020.

[16] E. Cusin, J. Honeine, M. Schieppati, and P. Rougier, "A simple method for measuring the changeable mechanical action of unloader knee braces for osteoarthritis," IRBM, vol. 39, no. 2, pp. 136-142, 2018.

[17] W. D. Lew, C. M. Patrnchak, J. L. Lewis, and J. Schmidt, "A comparison of pistoning forces in orthotic knee joints," Orthotics and prosthetics, vol. 36, no. 2, pp. 85-95, 1982.

[18] J. D. Hsu, J. Michael, and J. Fisk, AAOS Atlas of orthoses and assistive devices e-book. Elsevier Health Sciences, 2008.

[19] P. Walker, H. Kurosawa, J. Rovick, and R. Zimmerman, "External knee joint design based on normal motion," J Rehabil Res Dev, vol. 22, no. 1, pp. 9-22, 1985.
[20] S. Skals, R. Bláfoss, M. de Zee, L. L. Andersen, and M. S. Andersen, "Effects of load mass and position on the dynamic loading of the knees, shoulders and lumbar spine during lifting: a musculoskeletal modelling approach," Applied Ergonomics, vol. 96, p. 103491, 2021.
[21] H. Xu, S. Jampala, D. Bloswick, J. Zhao, and A. Merryweather, "Evaluation of knee joint forces during kneeling work with different kneepads," Applied ergonomics, vol. 58, pp. 308-313, 2017.
[22] B. A. Killen et al., "Automated creation and tuning of personalised muscle paths for OpenSim musculoskeletal models of the knee joint," Biomechanics and Modeling in Mechanobiology, vol. 20, no. 2, pp. 521-533, 2021.
[23] Y. Sun et al., "Study on the poroelastic behaviors of the defected articular cartilage," Computer Methods in Biomechanics and Biomedical Engineering, pp. 1-13, 2021.
[24] A. Javanfar and M. Bamdad, "Development of a planar multibody model of the knee joint with contact mechanics," Iranian Journal of Biomedical Engineering, 2022.
[25] M. Adouni, T. R. Faisal, and Y. Y. Dhaher, "Sensitivity analysis of the knee ligament forces to the surgical design variation during anterior cruciate ligament reconstruction: a finite element analysis," Computer Methods in Biomechanics and Biomedical Engineering, pp. 1-9, 2021.
[26] R. E. Richards, M. S. Andersen, J. Harlaar, and J. Van Den Noort, "Relationship between knee joint contact forces and external knee joint moments in patients with medial knee osteoarthritis: effects of gait modifications," Osteoarthritis and Cartilage, vol. 26, no. 9, pp. 1203-1214, 2018.
[27] A. Javanfar and M. Bamdad, " Knee Brace control for Reduction of Medial Compartment Load," in 2022 11th RSI International Conference on Robotics and Mechatronics (ICROM), 2022: IEEE, publishing.
[28] K. D. Gross and H. J. Hillstrom, "Noninvasive devices targeting the mechanics of osteoarthritis," Rheumatic Disease Clinics of North America, vol. 34, no. 3, pp. 755-776, 2008.
[29] R. Nisell, "Mechanics of the knee: a study of joint and muscle load with clinical applications," Acta Orthopaedica Scandinavica, vol. 56, no. sup216, pp. 1-42, 1985.
[30] R. L. Lenhart, J. Kaiser, C. R. Smith, and D. G. Thelen, "Prediction and validation of load-dependent behavior of the tibiofemoral and patellofemoral joints during movement," Annals of biomedical engineering, vol. 43, no. 11, pp. 2675-2685, 2015.
[31] M. Gao et al., "Design and optimization of exoskeleton structure of lower limb knee joint based on cross four-bar linkage," AIP Advances, vol. 11, no. 6, p. 065124, 2021.
[32] D. J. Hyun, H. Park, T. Ha, S. Park, and K. Jung, "Biomechanical design of an agile, electricity-powered lower-limb exoskeleton for weight-bearing assistance," Robotics and Autonomous Systems, vol. 95, pp. 181-195, 2017.
[33] B. Xiao, Y. Shao, and W. Zhang, "Design and optimization of single-degree-of-freedom six-bar mechanisms for knee joint of lower extremity exoskeleton robot," in 2019 IEEE International Conference on Robotics and Biomimetics (ROBIO), 2019: IEEE, pp. 2861-2866.
[34] Y. Sun, W. Ge, J. Zheng, and D. Dong, "Design and evaluation of a prosthetic knee joint using the geared five-bar mechanism," IEEE Transactions on Neural Systems and Rehabilitation Engineering, vol. 23, no. 6, pp. 1031-1038, 2015.
[35] A. Javanfar, and M. Bamdad. "A developed multibody knee model for unloading knee with cartilage penetration depth control." Proceedings of the Institution of Mechanical Engineers, Part H: Journal of Engineering in Medicine 236, no. 10 (2022): 1528-1540.
[36] A. Javanfar, and M. Bamdad. "Computational Control Strategy for Reducing Medial Compartment Load in Knee Bracing with Embedded Actuator." In Actuators, vol. 12, no. 6, p. 256. MDPI, 2023.
[37] A. Javanfar, and M. Bamdad. "Four-bar linkage mechanisms with continuous friction model in joint clearance." (2021).
[38] A. Javanfar. "Nonlinear Dynamic Behaviour of The Mechanisms Having Clearance and Compliant Joint." International Journal of Advanced Design & Manufacturing Technology 15, no. 4 (2022).
[39] A. Javanfar, H. M. Daniali, M. Dardel, and M. H. Ghasemi. "Dynamic behaviour analysis of four-bar linkage mechanisms with joints' clearance." In 2015 3rd RSI International Conference on Robotics and Mechatronics (ICROM), pp. 383-388. IEEE, 2015.
[40] A. Javanfar, and M. Bamdad. "Effect of novel continuous friction model on nonlinear dynamics of the mechanisms with clearance joint." Proceedings of the Institution of Mechanical Engineers, Part C: Journal of Mechanical Engineering Science 236, no. 11 (2022): 6040-6052.